Appl. Phys. B 81, 171–175 (2005)
DOI: 10.1007/s00340-005-1914-2

Applied Physics B
Lasers and Optics

Rapid communication

W. LEE✉
J.-S. GAU
H.-Y. CHEN

Electro-optical properties of planar nematic cells impregnated with carbon nanosolids

Department of Physics, Chung Yuan Christian University, Chung-Li, Taiwan 32023, Republic of China

Received: 15 October 2004 / Final version: 20 May 2005

ABSTRACT We report electro-optical effects in planar-aligned liquid-crystal cells of pristine and doped calamitics in the presence of dc voltage. The doped cells comprise both a nematic host and a minute amount of either buckminsterfullerene or multiwalled carbon nanotubes. The voltage–transmittance and voltage–capacitance hystereses were observed from the sample cells in the range of applied dc voltage up to 8 V. Experimental evidence indicates that a nanoscale carbon dopant can affect the behavior of a nematic in terms of ion-charge effects and that doping with nanotubes can effectively reduce the driving voltage.

PACS 42.70.Df; 42.79.Kr; 81.05.Tp; 82.70.Dd

1 Introduction

Nematic liquid-crystal (LC) displays are widely employed as an indispensable component in modern display devices due to many of their alluring features such as flatness, low power consumption and full color capability [1]. The performance of a LC device is greatly affected by the alignment layer and the LC material used. One of the most critical issues for nearly all the LC displays is the screening effect arising from the ionic impurities within the LC cell, because the ion-charge effect often results in flickering and image sticking and, in turn, in degradation of the image quality. Consequently, cyano compounds, such as 5CB and E7, known to have low resistivity and ion trapping near polyimide interfaces, are not employed in the thin-film-transistor-liquid-crystal-display (TFT–LCD) industry. For active-matrix displays the LC used must have high resistivity in order to avoid flickering and the voltage applied is ac, rather than dc, to avoid surface polarization, which would otherwise cause field-screening effects and degrade the display. Currently, a sufficiently high voltage-holding ratio can easily be achieved, thanks to the development of fluorinated LC substances and nearly contamination-free alignment materials.

One primary approach in conjunction with the emerging nanotechnology towards the improvement of performance of LC devices is structural modification of the LC host by nanoscale carbon additives [2–5]. Owing to their many unique physical, chemical and electronic properties, fullerenes and the allotrope carbon nanotubes (CNTs), a well-known family of nanomaterials, can widely be used as guest dopants in condensed optical materials to develop novel optoelectronic devices. Indeed, for instance, dramatic improvement of electro-optical characteristics has recently been observed in a *twisted nematic* (TN) liquid crystal by a minute addition of CNTs into the LC host [5].

In this paper, we further reveal the effects of the above-mentioned two types of carbon nanosolids on the electro-optical properties of a *planar-aligned* low-resistivity nematic LC in the presence of dc voltage. There are two basic reasons for our continuous efforts at exploring planar cells after the TN configuration. Firstly, a TN display with a total twist, say, $\pi/2$, much smaller than its phase retardation is sufficient for waveguiding along the twist, allowing the electric field vector to follow the nematic director as the beam propagates through the LC medium. This is known as the polarization-rotation effect. On the other hand, the electro-optical effect of a planar-aligned LC cell is achieved by the modulation of the total phase retardation, called the phase-retardation effect. Secondly, in a planar cell, only one (or maybe two in some cases) elastic constant is involved with both the threshold voltage and the rise and decay time constants, whereas all three elastic constants are involved for a twisted LC cell. In comparison with our previous work [5], we here provide detailed information on the sample ingredients and more insights into the working of the observed macroscopic effects. Similar studies for various LC modes (e.g. TN, planar-aligned, vertical-aligned, etc.) should be of help in understanding the mechanisms underlying the observed electro-optical effects. In order to highlight the influence of a carbon dopant in its small quantity on the behavior of a nematic in terms of the ion-charge effects, we elect to use a representative *low-resistivity* ($\sim 10^{11}\ \Omega$ cm) LC driven by a *dc* voltage for this study. The voltage–transmittance (V–T) and voltage–capacitance (V–C) hystereses as well as the switching curves were obtained from undoped, C_{60}-doped and CNT-doped LC cells. The experimental

---

✉ Fax: +886-(0)-3-265-3229, E-mail: wlee@phys.cycu.edu.tw

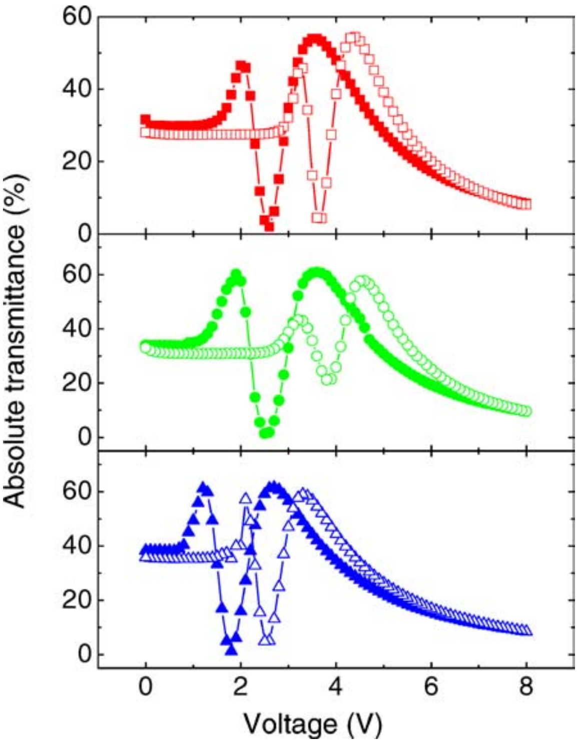

FIGURE 1 Transmittance vs. applied dc voltage and V–T hysteresis up to 8 V. The undoped cell, voltage up (■) and down (□); C_{60}-doped cell, voltage up (●) and down (○); CNT-doped cell, voltage up (▲) and down (△)

results indicate that doping a LC matrix with C_{60} will lower the dc threshold voltage and yet enhance the undesired charge-retention effects. However, doping LC with a trace of nanotubes will effectively suppress the ion-charge effect and, in turn, substantially reduce the dc threshold voltage to at least half that of an undoped planar cell.

2 Experimental

The basic sample fabrication approach was based on our previous work [2], which implied the concept of using liquid crystals to align carbon nanotubes parallel to the LC director. Empty cells were constructed from pairs of glass substrates separated by 5.7-μm ball spacers, yielding a cell gap of ∼ 6 μm. Both substrates in each pair were covered with indium–tin-oxide electrodes for application of an external dc field. The conducting substrates were then spin coated with polyimide to ensure a strong homogeneous alignment with a small tilt for our LC material. Assembly of each empty cell was accomplished to allow the directions of the rubbing on the substrates to be antiparallel to each other. The guest–host LC material was prepared from a suspension of either ultra-pure-grade (> 99.95%) fullerene C_{60} or purified open multiwalled CNTs (extract containing 90–95% nanotubes, of which 90% were uncapped at both ends) at a concentration of ∼ 0.01% by weight dispersed in the eutectic nematic E7. The CNTs we received consist of 18–25 concentric, cylindrical tubes of graphitic carbon with an average outer diameter of ∼ 10–20 nm and a length of 2–5 μm. It is worth mentioning that the fullerene C_{60} is zero-dimensional and semiconducting ($E_g = 1.9$ eV) and that the one-dimensional nanotubes we used are considered metallic ($E_g = 0$). Prior to their dispersion and ultrasonication in LC, carbon nanosolids were pretreated with a Wig-L-Bug grinding mill composed of a stainless steel vial and two agate ball pestles. Note that grinding helped prevent aggregation or physical entanglement and shortened the length of the CNTs [5]. To manufacture doped LC cells, the colloidal solution was introduced into the empty cells by capillary action at an elevated temperature well above the clearing point of E7, $T_c = 58.6$°C.

At low concentrations such as that adopted in this study, the clearing points of the suspensions were essentially not different from that of pure E7. Besides, compared with the counterparts filled with the neat LC, cells composed of either suspension were measured to possess the same value of the pretilt angle of 3.2 ± 0.5° within experimental error. The low concentration allowed the suspended nanosolids to be effectively separated in the LC hosts. The stability of the cells consisting of doped LCs, in terms of their electro-optical performance, was examined to assure their lifetime of more than a year. Unlike LC colloids containing networks of polymeric particles [6], optical polarizing microscopy cannot be utilized to characterize the morphology of the blends. The LC colloids of carbon nanosolids behaved as a pristine LC with no evidence of dissolved or precipitated particles.

The experimental setup for electro-optical measurements was primarily composed of a conventional geometry where the planar-aligned LC cell was placed between two crossed linear polarizers, with its (undisturbed) optical axis oriented at 45° with respect to the polarization of a low-power 633-nm He–Ne laser probe beam. A power supply provided dc bias voltage across the sample thickness. Because of the positive dielectric anisotropy ($\Delta\varepsilon \equiv \varepsilon_{\parallel} - \varepsilon_{\perp} > 0$) of the nematic E7, an electric field parallel to the sample thickness tends to reorient the nematic director and, hence, the optical axis toward the field direction; namely, homeotropically. To measure the electric capacitance, a LCZ meter running a small ac voltage of 50 mV at 1 kHz was used. The entire experimental system was interfaced with a personal computer via LabVIEW.

3 Results and discussion

Each data point in both Figs. 1 and 2 was taken 2 s after constant voltage was registered across the filled cell. To make it clear, the applied voltage increased step by step every two seconds up to 6 V and then decreased also step by step soon after with a measurement made at the end of each step. Figure 1 shows the absolute transmittance as a function of the dc voltage applied upon various cells at room temperature. As reference measurements without a LC cell, the absolute transmittance was measured to be ∼ 65%, ∼ 50% and ∼ 0.02% through solely the linear polarizer with its transmission axis parallel to the polarization of the incident laser beam, the parallel polarizers and the crossed

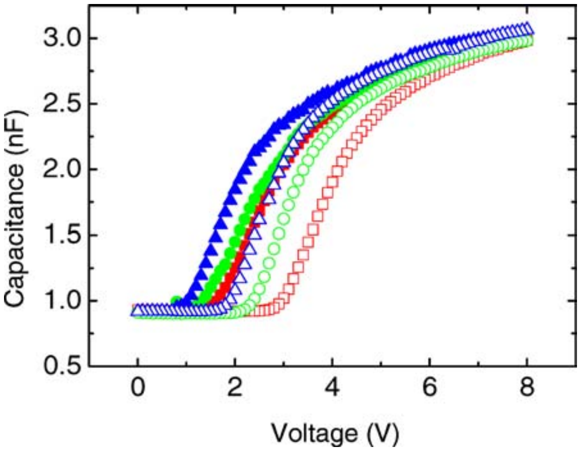

FIGURE 2 V–C hysteresis up to 8 V. The undoped cell, voltage up (■) and down (□); C_{60}-doped cell, voltage up (●) and down (○); CNT-doped cell, voltage up (▲) and down (△)

polarizers, respectively. The intensity of a probe beam traversing the polarizer–cell–analyzer system is given by [7]

$$I_\perp \propto I_0 \sin^2\left(\frac{\delta}{2}\right), \tag{1}$$

where I_0 denotes the incident polarized probe-beam intensity and δ stands for the phase retardation, which occurs due to the different propagating velocities of the ordinary and extraordinary rays in the cell. Note that the phase retardation can be calculated from the voltage-dependent transmitted intensity [8]. The oscillations in Fig. 1 clearly show that a director reorientation takes place in a direction different from the probe-beam polarization, leading to both ordinary and extraordinary waves inside the LC. This reorientation results in a phase retardation of a multiple of π, with each integer multiple of π corresponding to an extremum of the voltage-dependent transmittance. With an understanding of Eq. (1), one identifies that the valley, i.e. transmission minimum, corresponds to a phase retardation of 2π while the plateau at null voltage corresponds to a phase retardation of $\sim 3.5\pi$. The phase retardation can be expressed as

$$\delta = 2\pi d \Delta n/\lambda, \tag{2}$$

where d ($= 5.7\,\mu$m), λ ($= 633$ nm) and Δn ($= 0.220$ at 633 nm by a cubic spline fit [9]) denote the LC film thickness, probe-beam wavelength and effective LC birefringence, respectively. It is easy to show here that this formula gives the phase retardation near 4π for the cells under investigation in the absence of an applied voltage if the pretilt angle is ignored. Indisputably, the $T(V)$ curve is very sensitive to the wavelength although it is chosen to be 633 nm in this study.

If the threshold voltage V_{th} and the characteristic voltage $V_{2\pi}$ are defined as the voltages where the intensity transmitted is increased to 10% of the initial value at null voltage and decreased to the minimum, respectively, then it is clear from Fig. 1 that V_{th} $(V_{2\pi}) = 1.6$ (2.6), 1.2 (2.6) and 0.8 (1.9) V for the undoped, C_{60}-doped and CNT-doped cells, respectively. Although the dc threshold voltage is distinct from the well-recognized Fréedericksz threshold [10], V_{th} defined in this study is still presumably related to the first Oseen–Frank elastic constant K_{11} and to the square root of the dielectric anisotropy $\Delta\varepsilon$, i.e.

$$V_{\text{th}} \propto \sqrt{\frac{K_{11}}{\varepsilon_0 \Delta\varepsilon}}, \tag{3}$$

where ε_0 is the permittivity of free space. It is worth mentioning that, for a LC cell operating in the TN mode, $V_{\text{th}} \propto [(4K_{11} + K_{33} - 2K_{22})/\varepsilon_0\Delta\varepsilon]^{1/2}$, suggesting that the threshold of a TN cell is complicated by the involvement of all of the three Oseen–Frank elastic constants. Note that the effective dielectric anisotropy of the suspension can be approximated as [11]

$$\Delta\varepsilon_{\text{mix}} \approx (1-f)\Delta\varepsilon_{\text{LC}} + f\Delta\varepsilon_{\text{CNT}}, \tag{4}$$

where f stands for the fraction of CNTs. The apparent decrease in V_{th} for the CNT-doped cell, to just half that for the undoped counterpart, is partially attributed to the large dielectric anisotropy ($\Delta\varepsilon > 0$) of the high-aspect-ratio nanotubes and to the parallel orientation of the nanotubes to the LC director based on continuum theories as well as experimental verification [12]. Indeed, one can notice from Fig. 2 that the capacitance differences, when planar-aligned LC molecules are at rest ($\varepsilon_{\text{eff}} \approx \varepsilon_\perp$) and are in the high applied dc field ($\varepsilon_{\text{eff}} \approx \varepsilon_\parallel$), are distinct for the three types of cells. According to the relationship between the capacitance and the dielectric constant [5], one sees that CNT-doped E7 has to possess the smallest V_{th} because the tilt angles as well as the splay elastic constants are considered identical for these cells.

Owing to the field-screening effect, the above discussion with Fig. 2 can only be regarded as indirect evidence for the increase in dielectric anisotropy. To quantitatively verify the increase in the dielectric anisotropy, we conducted an independent experiment involving the transient current in a LC cell induced by the dc switch of a step voltage [13]. Let us consider the one-dimensional distribution of a nematic director $\mathbf{n} = (\cos\theta(t), 0, \sin\theta(t))$ in a uniform electric field along the cell thickness, where $\theta(t)$ is the tilt angle between an alignment layer surface and the director. The effective dielectric constant $\varepsilon_{\text{eff}}(\theta(t))$, given by

$$\varepsilon_{\text{eff}}(\theta(t)) = \varepsilon + \Delta\,\varepsilon \sin^2\theta(t), \tag{5}$$

increases with increasing applied voltage $V (\gg V_{\text{th}})$ due to the reorientation of the nematic director to minimize the total free energy. Using the concept of a parallel-plate capacitor, the dielectric anisotropy can be determined by the slope of the additional charge Q as a function of V in accordance with

$$Q = \frac{(\varepsilon_0 \Delta\varepsilon \sin^2\theta)A}{d} V, \tag{6}$$

where A is the area of the cell and d, again, is the cell gap. We obtained the value of Q by measuring transient current in a step voltage and then by integrating the transient current with time. The dielectric anisotropy of the CNT (0.05 wt.%) suspension was therefore measured via $\Delta\varepsilon_{\text{mix}} = (Q_{\text{mix}}/Q_{\text{LC}})\Delta\varepsilon_{\text{LC}}$, giving a value of 1.1 times greater than that of the pure nematic E7 [14]. Because the V_{th} ratio of the CNT-doped cell to the undoped cell, estimated by $(\Delta\varepsilon_{\text{LC}}/\Delta\varepsilon_{\text{mix}})^{1/2}$, is only 0.95, the deduced reduction is so limited that it can hardly account for the dramatic decrease in dc threshold voltage observed in CNT-doped cells. With the experimental

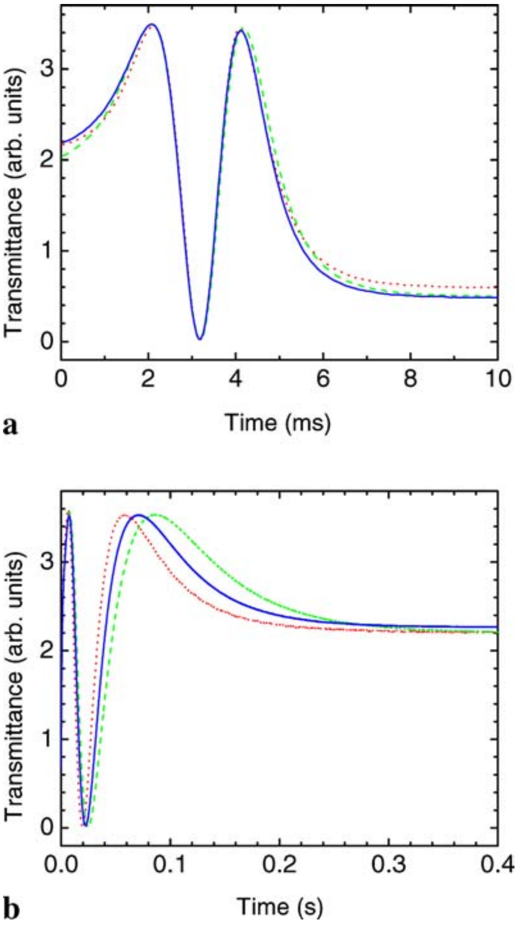

FIGURE 3 Optical transmission upon electrical switching **a** on to 6 V and **b** off from 6 V. The undoped cell, *dotted line*; C_{60}-doped cell, *dashed line*; CNT-doped cell, *solid line*

results obtained from our most recent study of electro-optical properties in CNT-doped cells driven by an *ac* voltage [15], we believe that the phenomena observed in this study are best explained by the involvement of CNTs as a dopant whose interaction with ion impurities permitted the thinness of the effective electric bilayers and, in turn, allowed the nematic molecules in the doped cell to experience a relatively higher effective external field for the same dc voltage applied and thus led to the subsequent lowering of the driving voltage assisted by the increased dielectric anisotropy. In other words, the most important contribution to the reduction of the dc threshold voltage was the suppression of the screening effect by the addition of CNTs dispersed in E7. This will be discussed later. It is likely that the carbonaceous additives, in spite of their trace amount, modified the LC/polyimide interface and thus lowered the anchoring strength. (The weak anchoring gives rise to a lower threshold based on $V_{\text{th}} = \pi(K_{11}/\varepsilon_0\Delta\varepsilon)^{1/2}/(1 + 2K_{11}/W_\theta d)$, where W_θ is the polar anchoring energy.) Indeed, because the surface electric bilayers were explicitly associated with the surface-charge field, one could not undoubtedly say that the anchoring energy was not modified by the ion-binding process [16].

Figure 1 also illustrates the V–T hysteresis due to the field-screening effect of the ion charges. It is worth mentioning that, with a constant field, the screening effect decreases continuously the field inside the LC. Thus, hysteresis must depend on the time (here 2 s) for which the constant voltage is applied and on the voltage difference between two measurements. Here, in Fig. 1, the hystereses at $\delta = 2\pi$ are 1.1, 1.2 and 0.6 V for the undoped, C_{60}-doped and CNT-doped cells, respectively. Noticeably, the hysteresis of the CNT-doped cell reduces to nearly half that for the undoped one. It is obvious that the cell filled with the CNT suspension exhibits the smallest voltage offset, indicating that the CNT dopant detracts the severe ion-charge effects caused by residual ionic impurities in the neat nematic E7. As a matter of fact, the ion charges often originate in impurities in the LC itself or from foreign dopants. The screening effect, owing to the increased population of adsorbed ion charges on the interfaces under an applied dc voltage, results in a decrease of the effective voltage. Apparently, the C_{60}-doped cell suffers from more severe field-screening effects as shown in Fig. 1.

Figure 2 shows the capacitance variation in the undoped and doped cells. The capacitance of planar-aligned nematic cells rises with increasing voltage in that the nematic adopted has a positive dielectric anisotropy. This figure demonstrates that the V–C hysteresis of the CNT-doped cell is less serious than that of the undoped cell. Despite the relatively narrow hysteresis width of the C_{60}-doped cell in comparison with that of the undoped counterpart, the general behaviors revealed by Fig. 2 are consistent with the previous observation.

Figure 3a displays the dynamic response of LC after the externally applied voltage is switched on to 6 V. While a dc voltage of 6 V is applied to the cells, the LC molecules are aligned into the steady quasi-homeotropic state and the darker state is obtained. Each time-evolved transmittance curve during the response time mimics the shape of the voltage-dependent transmittance as shown in Fig. 1. Note that the rise and decay times of a planar-aligned LC display cell may be given by the mathematical expression

$$t_{\text{switching}} \propto \frac{\gamma_1 d^2}{\varepsilon_0 \Delta\varepsilon V^2 - \pi^2 K_{11}}, \qquad (7)$$

where γ_1 is the rotational viscosity. As $\pi^2 K_{11}$ is very small compared with $\varepsilon_0\Delta\varepsilon V^2$, the rise time and decay time are given mainly by $T_{\text{rise}} \propto \gamma_1 d^2/\varepsilon_0\Delta\varepsilon V^2$ and $T_{\text{decay}} \propto \gamma_1 d^2/K_{11}$, respectively. One can see from Fig. 3a that, because the rise time is strongly dependent on the switching voltage V ($\gg V_{\text{th}}$), little difference exists between the response curves corresponding to the undoped and doped cells. Figure 3b depicts the dynamic response of LC relaxation, which is measured as transmittance vs. time after the dc voltage is switched off. The relaxation curves between the distinct LC cells are clearly distinguishable. Obviously, a carbon-nanosolid additive slows down the relaxation process. It is known that the concentration of dichroic dyes for guest–host LC displays is often very low to avoid the increase of γ_1. It is reasonable to suspect that the CNT doping increased the rotational viscosity in the nematic system. However, its minute amount ($\sim 0.01\%$ by weight) would result in very limited amendment of the viscosity as well as the viscoelastic coefficient γ_1/K_{11}. Indeed, our transient-current experiment mentioned above led to the rotational viscosity of the CNT (0.05 wt%) suspension of 0.039 Pa s, a value comparable to that of pristine E7 of 0.035 Pa s [14]. One should be reminded that the optical decay time is proportional to $(\gamma_1/K_{11})d^2$ for strong anchoring ($W \to \infty$) while it is proportional to $\gamma_1 d/2W$ for a weak-anchoring boundary condition. Because the relaxation time constants of the neat and nanotube-doped nematic cells are only slightly different, no readily apparent evidence is found for an appreciable reduction of anchoring energy due to considerable modification (if any) of the LC/polyimide interface by doping with CNTs.

4 Conclusion

In summary, dc electro-optical properties have been examined in planar-aligned nematic liquid-crystal cells doped with carbon nanosolids—buckminsterfullerene or multiwalled carbon nanotubes. Experimental results indicate that the nanoscale carbon dopant, even in its minute amount, influences the effective dc voltage on the LC bulk and director-orientation characteristics. CNT-doped cells are distinguished in this investigation. The preliminary data cannot provide strong evidence for any substantial modification of the LC/polyimide interface by CNTs, which would weaken the anchoring strength and, in turn, lower the threshold voltage. The apparent reduction in V_{th} for the CNT-doped cell is attributed primarily to the suppression of the field screening and secondarily to the increase of the dielectric anisotropy by the addition of the high-aspect-ratio nanotubes oriented preferably in parallel to the LC director. To obtain a full understanding of the observed effects reported in this work requires extensive experimental data of material characteristics and cell parameters, including the anchoring strength. A detailed study of the mechanisms underlying the observed decrease in V_{th} is currently being pursued in this laboratory.

ACKNOWLEDGEMENTS We gratefully acknowledge support from the National Science Council of the Republic of China (NSC-92-2112-M-033-008).

REFERENCES

1 E. Lueder, *Liquid Crystal Displays: Addressing Schemes and Electro-Optical Effects* (Wiley, New York, 2001)
2 W. Lee, C.-S. Chiu, Opt. Lett. **26**, 521 (2001)
3 W. Lee, Y.-L. Wang, Chin. J. Phys. (Taipei) **39**, L295 (2001)
4 M. Suzuki, H. Furue, S. Kobayashi, Mol. Cryst. Liq. Cryst. **368**, 191 (2001)
5 W. Lee, C.-Y. Wang, Y.-C. Shih, Appl. Phys. Lett. **85**, 513 (2004)
6 M.C.W. van Boxtel, R.H.C. Janssen, C.W.M. Bastiaansen, D.J. Broer, J. Appl. Phys. **89**, 838 (2001)
7 M. Born, E. Wolf, *Principles of Optics*, 7th edn. (Cambridge University Press, New York, 1999), Chap. 15
8 I.C. Khoo, S.T. Wu, *Optics and Nonlinear Optics of Liquid Crystals* (World Scientific, Singapore, 1993), Chap. 2
9 R.L. Sutherland, V.P. Tondiglia, L.V. Natarajan, T.J. Bunning, W.W. Adams, Appl. Phys. Lett. **64**, 1074 (1994)
10 L.M. Blinov, *Electro-Optical and Magneto-Optical Properties of Liquid Crystals* (Wiley, New York, 1983)
11 Y. Reznikov, O. Buchnev, O. Tereshchenko, V. Reshetnyak, A. Glushchenko, J. West, Appl. Phys. Lett. **82**, 1917 (2003)
12 M.D. Lynch, D.L. Patrick, Nano Lett. **2**, 1197 (2002) and references therein
13 O. Nakagawa, M. Imai, H. Naito, A. Sugimura, Jpn. J. Appl. Phys. **35**, 2762 (1996)
14 H.-Y. Chen, W. Lee, in preparation
15 W. Lee, Y.-C. Shih, to appear in J. Soc. Inf. Disp. **13** (2005)
16 G. Barbero, L.R. Evangelista, N.V. Madhusudana, Eur. Phys. J. B **1**, 327 (1998)